Journal of Aerosol Science 78 (2014) 41–54

Contents lists available at ScienceDirect

Journal of Aerosol Science

journal homepage: www.elsevier.com/locate/jaerosci

Generation, inhalation delivery and anti-hypertensive effect of nisoldipine nanoaerosol

A.A. Onischuk [a,b,*], T.G. Tolstikova [b,c], A.M. Baklanov [a], M.V. Khvostov [c], I.V. Sorokina [c], N.A. Zhukova [c], S.V. An'kov [c], O.V. Borovkova [a], G.G. Dultseva [a,b], V.V. Boldyrev [b,d], V.M. Fomin [b,e], G. Steven Huang [f]

[a] Institute of Chemical Kinetics & Combustion, RAS, Novosibirsk 630090, Russia
[b] Novosibirsk State University, Novosibirsk 630090, Russia
[c] Institute of Organic Chemistry, RAS, Novosibirsk 630090, Russia
[d] Institute of Solid State Chemistry & Mechanochemistry, RAS, Novosibirsk 630090, Russia
[e] Institute of Theoretical and Applied Mechanics, RAS, Novosibirsk 630090, Russia
[f] Department of Materials Science and Engineering, National Chiao Tung University, 1001 University Road, Hsinchu, Taiwan, ROC

ARTICLE INFO

Article history:
Received 22 May 2014
Received in revised form
11 August 2014
Accepted 13 August 2014
Available online 2 September 2014

Keywords:
Evaporation–nucleation route
Nanoerosol lung deposition
Pulmonary delivery
Nisoldipine

ABSTRACT

Nisoldipine is a dihydropyridine subclass calcium channel blocker with low oral bioavailability. Therefore, novel drug delivery systems able to enhance nisoldipine bioavailability are urgently needed. Here the nanoaerosol pulmonary administration of nisoldipine is investigated in experiments with WISTAR and ISIAH rats. The drug aerosol inhalation scheme includes an evaporation–condensation aerosol generator, inhalation chambers for rats, and aerosol spectrometer (to control aerosol concentration and size distribution). The particle mean diameter and number concentration are within the ranges 10–200 nm and 10^3–2×10^7 cm^{-3}, respectively. The chemical composition of nanoaerosol particles was shown by means of liquid chromatography to be identical with the maternal drug. Using nose-only exposure chambers, the rat lung deposition efficiency was evaluated as a function of particle diameter. The dose-dependent effect from aerosolized nisoldipine was compared with that from the intravenous and oral drug delivery. In particular, it was found that nisoldipine aerosol administration is essentially more effective than traditional oral treatment, i.e. it gives the same blood pressure reduction as the oral treatment at the body deposited dose about 100 times less.

1. Introduction

Pulmonary system is an attractive target for drug delivery. Nowadays aerosolized therapeutics is widely used to treat local lung diseases such as asthma, emphysema, chronic obstructive pulmonary disease, cystic fibrosis, primary pulmonary hypertension, and cancer (Bailey & Berkland, 2009; Gagnadoux et al., 2005; Ruge et al., 2013). Treating these diseases locally is advantageous since the drug avoids first-pass metabolism and deposits directly at the disease site. This type of drug

* Corresponding author at: Institute of Chemical Kinetics and Combustion, Russian Academy of Sciences, Siberian Branch, Institutskaya, 3, Novosibirsk 630090, Russia. Tel.: +7 383 3333244; fax: +7 383 3307350.
E-mail address: onischuk@kinetics.nsc.ru (A.A. Onischuk).

http://dx.doi.org/10.1016/j.jaerosci.2014.08.004
0021-8502/

application to lung epithelium also eliminates potential side effects caused by high systemic concentrations typical for conventional drug delivery methods, and can reduce costs because smaller doses can be used. In addition, the lung alveolar part is increasingly considered as a portal of entry for aerosolized drugs designed to act systemically (Agu et al., 2001; Labiris & Dolovich, 2003; Laube, 2005; Patton et al., 2004). Large surface area, good vascularization and ultra-thinness of alveolar epithelium (0.1–0.2 μm) are unique features of lungs that can facilitate systemic delivery *via* pulmonary administration. Lungs are far more permeable to drugs than any other portal of entry into the body. Inhalation is a fast way to get into the body because drug efflux transporters and metabolizing enzymes are present in lungs at much lower levels than in gastrointestinal tract (Patton et al., 2004). In contrast to injection therapy, inhalation therapy is non-invasive and, therefore, is not associated with pain, so this should improve patient comfort and compliance. Besides, there is no risk of needle injuries, no need for health-care staff, and patients are able to use this method at home. Drug nanoparticles must dissolve for the substance to be absorbed after inhalation. Small molecules are absorbed extremely rapidly, about one minute for lipophilic molecules (Patton et al., 2004; Rabinowitz et al., 2004) and a few tens of minutes for water-soluble ones (Patton et al., 2004). Therefore, the inhalation way of drug administration can be used to treat a variety of symptoms that beg for a quick response.

However, the treatment of systemic diseases through the inhalation route is hampered by uncertainties of the drug dose applied by inhalation. The dose depends on many factors including particle size and dissolution time. The particles 10–20 nm in size deposit to the alveolar region about 4 times more efficiently than those several microns in diameter (Edwards et al., 2003; Hinds, 1999; Heyder, 2004; Hussain et al., 2011; Jaques & Kim, 2000; Labiris & Dolovich, 2003; Oberdörster et al., 2005; Wong, 2007). On the other hand, dissolution time for nanosized particles is essentially shorter than for micron-sized ones. In other words, the lung delivered dose accuracy is higher for nanosized particles with respect to that for micron sized ones. Thus, better delivery devices are to be developed to produce small-particle aerosols allowing high drug doses to be deposited in the alveolar region of lungs where they are available for systemic absorption. A promising way for the generation of small drug particles in high concentration is the evaporation–nucleation technique (Onischuk et al., 2008, 2009; Rabinowitz et al., 2004, 2006; Rabinowitz & Zaffaroni, 2004; Tolstikova et al., 2013). This technique allows generating nanoaerosol within the mean diameter range from 5 to 500 nm and with the number concentration of particles up to $10^8\,cm^{-3}$. In particular, this way of nanoaerosol synthesis was demonstrated to be effective for a variety of drug substances (Rabinowitz et al., 2004, 2006; Rabinowitz & Zaffaroni, 2004). In our previous publications (Onischuk et al., 2008, 2009; Tolstikova et al., 2013) we elaborated an approach for evaporation–nucleation nanoaerosol delivery in mice. It was demonstrated for non-steroid anti-inflammatory drugs that the inhalation route is much more effective than traditional oral therapy.

Cardiovascular diseases are by far the most frequent causes of death in industrialized countries. Hypertension affects about 600 million people worldwide (Babatsikou & Zavitsanou, 2010). Among others, calcium antagonists are widely used to treat hypertension. Amid the calcium antagonist class, drugs in dihydropyridine subclass are effective antihypertensive agents, and their use has been shown to improve cardiac and cerebrovascular outcome in clinical trials (White, 2007). Nisoldipine is a dihydropyridine subclass calcium channel blocker with low oral bioavailability. This was attributed to slow dissolution and presystemic metabolism (Maghraby & Elsergany, 2014). Accordingly, the objective of many scientific contributions was to enhance nisoldipine bioavailability. In particular, novel drug delivery systems can provide a chance for the drug to escape from metabolism (Prisant & Elliott, 2003).

In this paper we propose the nanoaerosol inhalation way of nisoldipine delivery. We study the anti-hypertension effect from the nanoaerosol form of nisoldipine in inhalation experiments with laboratory rats. The evaporation–nucleation way is used to generate nisoldipine nanoparticles. Essential efforts are concentrated here on developing the method of inhalation dose measurement. A decrease in blood pressure due to inhalation is compared with the effect from intravenous (i.v.) injection and traditional oral drug administration.

2. Materials and methods

The principle of nisoldipine nanoaerosol generation is shown in Fig. 1. The generator consists of a cylindrical flow chamber heated outside and charged with nisoldipine substance. Filtered air is supplied to the inlet of the generator. Saturated vapor is formed inside the generator. As the air saturated with nisoldipine vapor moves along the tube, temperature drops down at the outlet of the heated zone resulting in vapor supersaturation. Due to homogeneous nucleation, aerosol particles are formed from supersaturated vapor. Two kinds of nisoldipine generators are elaborated in

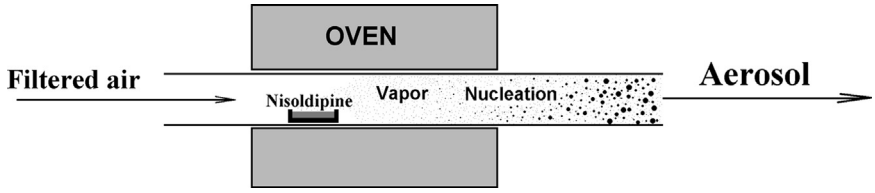

Fig. 1. Scheme of the evaporation–nucleation method of nanoaerosol formation.

the framework of this study: the laboratory one (Fig. 2) with the length of 60 cm, aimed at inhalation experiments with laboratory rats or mice, and a portable inhaler (Fig. 3) aimed at the use by people. All the following experiments with laboratory animals are carried out using the laboratory nanoaerosol generator.

The inhalation scheme includes a flow aerosol generator, inhalation chambers for rats, and an aerosol spectrometer to measure nanoaerosol concentration and size distribution (Fig. 4). The horizontal evaporation–nucleation aerosol generator is made of a molybdenum glass tube (of inner diameter 1.0 cm) with an outer heater. Air is supplied to the inlet of the generator through the Petrianov's high efficiency aerosol filter (Kirsh et al., 1975) with the flow rate $Q_g = 8.0\ \mathrm{cm}^3/\mathrm{s}$ (at standard temperature and pressure). The original substance (nisoldipine BG0270) is placed in the hot zone inside the tube. Saturated vapor is formed inside the generator. The outgoing aerosol is monitored with the aerosol spectrometer designed and built at the Institute of Chemical Kinetics and Combustion, Novosibirsk, Russia (Ankilov et al., 2002). The aerosol spectrometer consists of an automatic diffusion battery, condensation chamber and photoelectric counter.

Fig. 2. Laboratory generator of drug nanoaerosol.

Fig. 3. Portable evaporation–nucleation inhaler intended for humans.

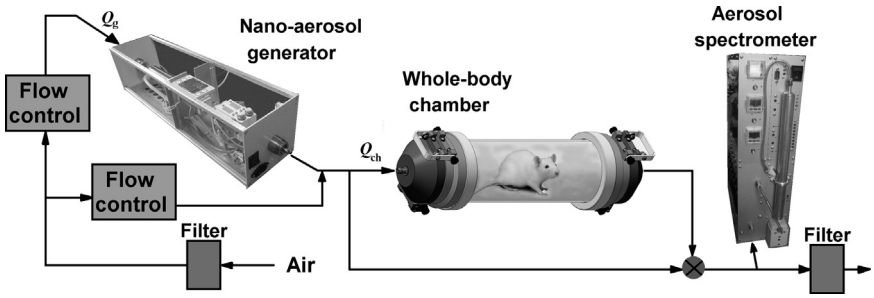

Fig. 4. Scheme of the experimental set-up.

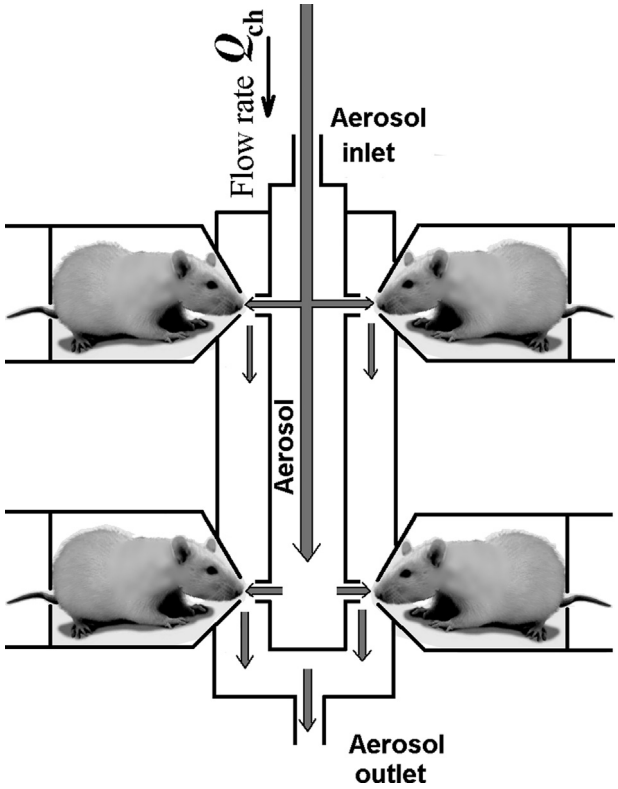

Fig. 5. Scheme of the "nose-only" inhalation experiments.

This device is able to measure particle size distribution within the range 3–200 nm and aerosol concentration within the range 10^1–5×10^5 cm^{-3} directly and up to 10^9 cm^{-3} using the aerosol dilution technique. A three-cascade diluter is used to measure particle concentration in the range 10^5–10^9 cm^{-3}. The first cascade unit is to decrease the aerosol concentration by mixing the aerosol with pure air. For this purpose, an ejecting system or just a three-way mixing junction is used. The other two cascades section splits the aerosol flux into two ones; one of these is filtered and then the fluxes are mixed again. The first cascade unit gives the dilution ratio 10–100 and the other two cascades section provides the dilution coefficient of 100.

The aerosol flux is mixed with pure air at the outlet of generator (with the ratio of 1:9, respectively) and then supplied with the flow rate $Q_{ch}=80$ cm^3/s to inhalation chambers. Both whole-body (WB) and nose-only exposure (NOE) inhalation chambers are used in inhalation experiments. The WB chamber is made of quartz cylinder with the length of 40.0 cm and inner diameter 9.0 cm; it is equipped with two opposite side stainless steel hatches (see Fig. 4). A single rat was housed in the WB chamber during the inhalation. The rat was free to move along the WB chamber during the aerosol exposure. Both WISTAR (normal blood pressure) and ISIAH (Inherited Stress Induced Hypertension, elevated blood pressure) rats were used in aerosol exposure experiments. The body weight (bw) was 200 ± 10 g for WISTAR and 350 ± 20 g for ISIAH rats. The NOE inhalation set-up is schematized in Fig. 5. The latter set-up is furnished with four ports to be socketed with glass rat chambers. The temperature in both the WB and the NOE chambers was 295 K, which corresponded to the room temperature, and relative humidity was in the range 50–70%. Inhalation time in all the experiments was 40 min. The experiments with rats were provided in the Laboratory of Pharmacological Research (Institute of Organic Chemistry, Russian

Academy of Sciences, Novosibirsk) which was accredited as satisfying to the international standards ISO/IEC 17025-2000, approval code ROSS RU.0001.514430; No. 000269. All studies were carried out in accordance with the Guideline for the Care and Use of Laboratory Animals (Geneva Convention for the Protection of Animals, 1986).

The inhaled dose was measured in separate experiments. NOE exposure glass chambers were used to minimize the skin or fur effects. Four chambers were arranged in series. The laboratory animals were confined so that only nose was exposed to the aerosol (Figs. 6 and 7). The aerosol flow rate through the chamber series was set at $Q_d = 17$ cm^3/s in the inhalation dose measurement experiments.

Chromatographic analysis of aerosol particles was performed to make sure that there was no thermal decomposition or oxidation of nisoldipinne during evaporation–condensation. For this purpose, aerosol particles were sampled by passing the aerosol flux through the Petrianov high-efficiency aerosol filter. Then the deposit was dissolved in acetonitrile. The high-performance liquid chromatograph Milikhrom A-02 (EcoNova, Novosibirsk, Russia) equipped with a UV-spectrophotometric detector was used. Chromatographic column (⌀2.0 × 75 mm, filled with reverse-phase sorbent ProntoSIL 120-5-C18 AQ #1810, grain diameter 5 μm) was thermostated at a temperature of 308 K. Elution was carried out with a mixture of acetonitrile (grade 0) with distilled water in the gradient 20–80% (acetonitrile). Elution rate was 100 μl/min, detection was performed at the wavelength of 236 nm. The volume of sample introduced into the column was 2 μl.

The hypotensive effect from inhalation-administrated drug was compared with the blood pressure decrease after the i.v. injection and oral treatment. Both the injections and oral delivery were done using nisoldipine emulsion in water stabilized by Tween 80. In the cases of inhalation and oral treatments, the arterial blood pressure was measured before and after the drug delivery (4 min after inhalation and 40 min after oral delivery) by means of the tail-cuff method using the LE 5007 Automatic Blood Pressure Computer (Panlab, Spain) allowing readings when pulse/flow disappears during cuff inflation and reappears during deflation, separated by a compression interval. In the case of i.v. injections, the blood pressure was measured before and 4 min after the treatment by the carotid artery cannulation method using a Coulbourn Lablink V system (the rats were anesthetized with sodium thiopental, 30 mg/kg bw).

A histologic analysis was performed to observe the effect of nisoldipine aerosol on the rats' lung morphology. The rats were killed 6.3 h after the exposure. Lungs were fixed in 10% paraformaldehyde in the phosphate buffer (pH 7.2–7.4). The fixed tissues were treated in a standard way using the "MICROM" histological equipment (Carl Zeiss) and then embedded in paraffin. Sections 3–4 μm thick were stained with hematoxylin and eosin. Slides were examined under the light microscope Axioskop 40 (Carl Zeiss).

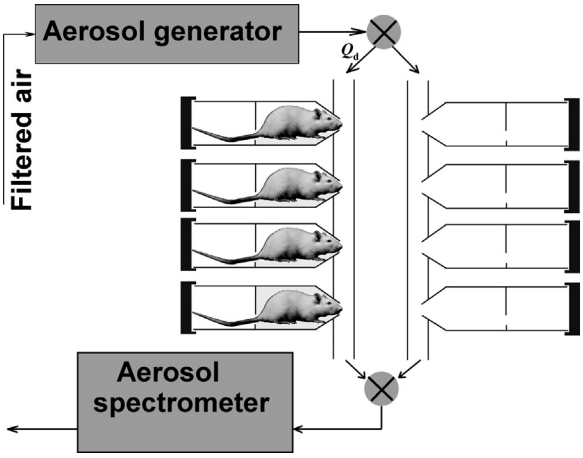

Fig. 6. Scheme of the inhaled dose measurement experiment.

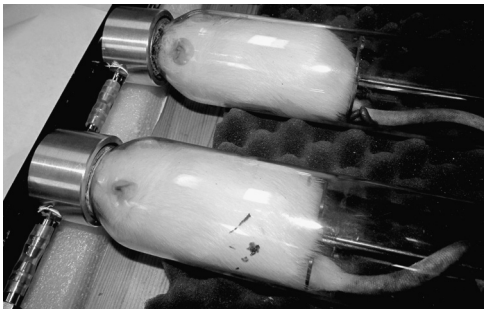

Fig. 7. View of the nose-only exposure chambers connected in series for the inhaled dose measurements.

3. Results and discussion

3.1. Aerosol size, concentration, and composition

A typical aerosol diameter distribution as measured at the outlet of aerosol generator is shown in Fig. 8. The particle size distribution is well approximated by the log-normal function f with the standard geometric deviation $\sigma_g = 1.4$:

$$f = \frac{1}{\sqrt{2\pi} d \ln \sigma_g} \exp\left\{ -\frac{1}{2}\left(\frac{\ln(d/d_m)}{\ln \sigma_g} \right)^2 \right\} \quad (1)$$

where d and d_m are the diameter and geometric mean diameter, respectively.

The aerosol number concentration and arithmetic mean diameter d_a are shown in Figs. 9 and 10 as functions of the generator temperature T. The typical range of aerosol concentration is 10^3–2×10^7 cm^{-3}. At $T > 425$ K, the aerosol

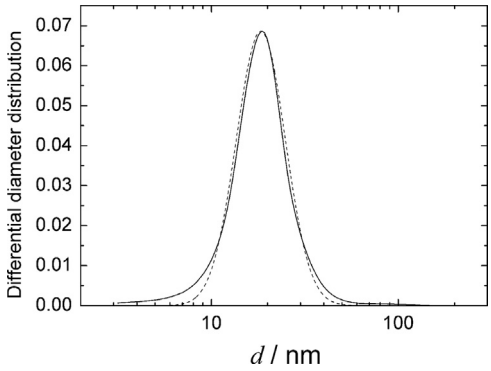

Fig. 8. Solid line – typical aerosol diameter distribution as measured at the outlet of laboratory aerosol generator; dash line – log-normal function (standard geometric deviation $\sigma_g = 1.4$).

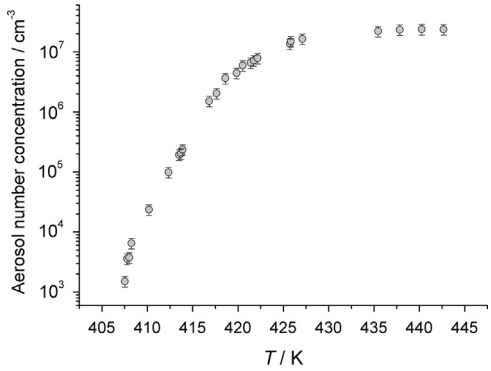

Fig. 9. Aerosol number concentration at the outlet of aerosol generator vs. the evaporation temperature.

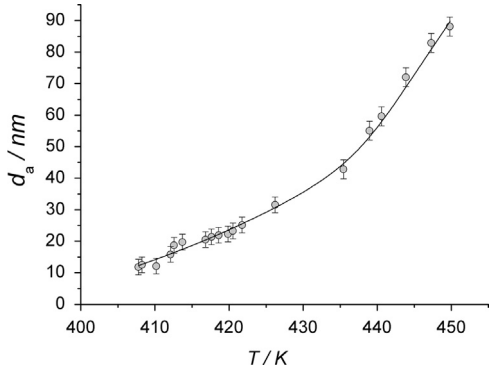

Fig. 10. Aerosol arithmetic mean diameter vs. the evaporation temperature. Solid line is an eye guide.

concentration asymptotically approaches the value $C_{lim} \approx 2 \times 10^7\ \mathrm{cm}^{-3}$. This limiting value is governed by aerosol coagulation (Fuchs, 1964):

$$C_{\mathrm{lim}} \approx \frac{1}{k\tau} \tag{2}$$

where k is the coagulation rate constant, τ is the aerosol residence time, i.e. the mean time between nucleation and aerosol dilution before measurement with the aerosol spectrometer. The aerosol mean diameter increases progressively with increasing temperature (see Fig. 10) as the vapor pressure in the evaporation zone is an exponential function of temperature.

Chromatographic analysis showed that the chromatogram from nanoparticles was identical to that from the original nisoldipine sample (Fig. 11).

3.2. Lung-deposited dose

A fundamental requirement in animal aerosol inhalation studies is that the lung-delivered dose is to be known. The dose measurements were provided using four nose-only chambers joined in series (Fig. 7). Two lines, loaded with rats and unloaded one, were set in parallel (Fig. 6). The aerosol concentration was monitored by turn at the outlets of the loaded and unloaded NOE lines (see Fig. 12). The fraction α of particles consumed per chamber due to rat breathing was determined via expression (Onischuk et al., 2009):

$$\alpha = 1 - \left(\frac{n_{out}}{n_{out}^{(0)}}\right)^{1/N} \tag{3}$$

where n_{out} and $n_{out}^{(0)}$ are aerosol number concentrations as measured by the aerosol spectrometer at the outlets of the loaded and unloaded NOE lines, respectively, N is the number of chambers in the tandem.

The rate D [s^{-1}] of particle lung deposition per rat can be written as (Onischuk et al., 2009)

$$D \approx Q_d \alpha n_{av}, \tag{4}$$

where Q_d (cm^3/s) is flow rate through the NOE chambers tandem and n_{av} is the arithmetic mean between the loaded NOE line inlet and outlet particle concentrations. Using the function D we determined the lung-deposited dose (weight of the lung-deposited particles per rat):

$$Dose = Dmt \tag{5}$$

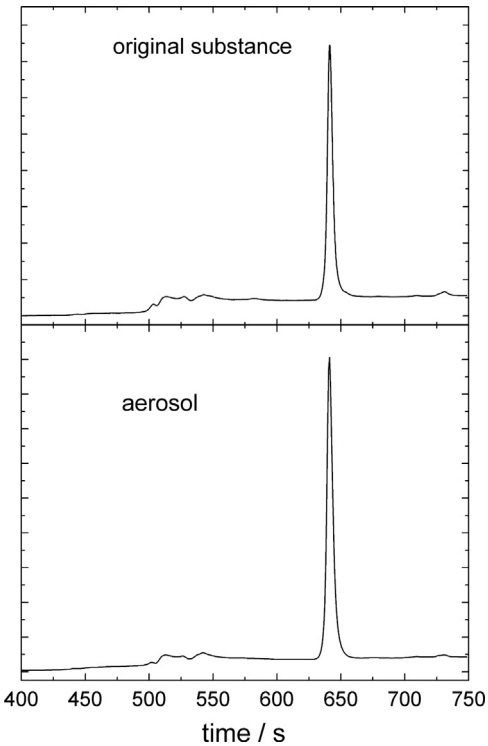

Fig. 11. Comparison between the chromatograms of original nisoldipine powder and nanoparticles (with the mean diameter of 60 nm) formed by evaporation–nucleation.

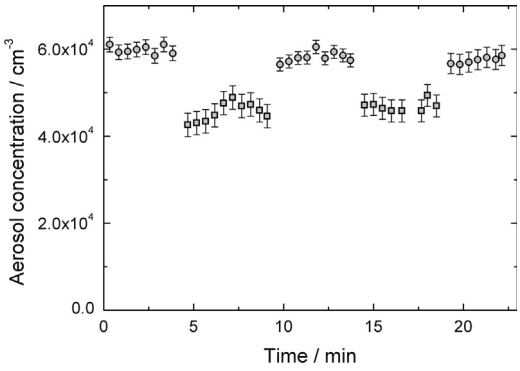

Fig. 12. Aerosol number concentration as measured consecutively with the aerosol spectrometer at the outlets of the loaded (squares) and unloaded (circles) NOE lines vs. laboratory time. WISTAR rats were used.

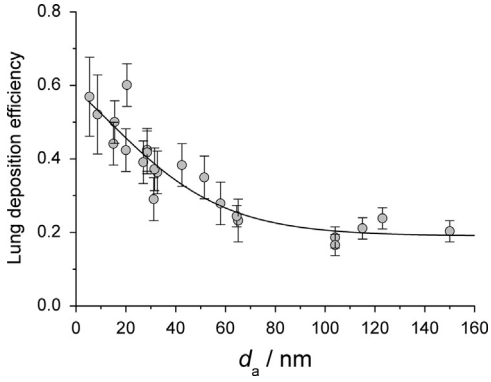

Fig. 13. Lung deposition efficiency vs. the mean diameter of nisoldipine particles. Line is an eye guide.

where m is the mean mass of aerosol particles, t is the inhalation time (s). To be able to determine the lung-deposited dose in any other inhalation chamber, one should know total lung deposition efficiency ε, i.e. the difference between the numbers of inhaled and exhaled particles divided by the number of inhaled ones. This deposition efficiency can be determined from the following evident relationship:

$$60Q_d\alpha \approx \dot{V}_E\varepsilon \tag{6}$$

where $\dot{V}_E$ (cm^3/min) is the minute volume (the factor 60 is used to recalculate minutes to seconds). The recommended minute volume for rats can be estimated as (Arms & Travis, 1988)

$$\dot{V}_E\,(\mathrm{cm}^3/\mathrm{min}) \approx 490*(\mathrm{bw/kg})^{0.75} \tag{7}$$

Finally, from Eqs. (3) and (6) we get

$$\varepsilon \approx \frac{60Q_d}{\dot{V}_E}\left[1-\left(\frac{n_{out}}{n_{out}^{(0)}}\right)^{1/N}\right]. \tag{8}$$

The total lung deposition efficiency as determined from the experimental measurement of n_{out} and $n_{out}^{(0)}$ is shown in Fig. 13 as a function of the mean particle diameter. One can see that ε tends to about 0.6 at small diameter values, which is in a reasonable agreement with numerical simulations for the particle deposition in the airways of rats (Hofmann et al., 2000). The function $\varepsilon(d)$ is well approximated by the Boltzmann sigmodal function (see solid line):

$$\varepsilon(d/\mathrm{nm}) = A_2 + (A_1 - A_2)\Big/\left(1+\exp\left(\frac{d-d_0}{\delta d}\right)\right) \tag{9}$$

with $A_1=0.83$; $A_2=0.19$; $d_0=12.0$ nm; $\delta d=24.0$ nm.

Now it is possible to estimate the lung-deposited dose in any other inhalation chamber *via* the expression:

$$Dose = \frac{\dot{V}_E}{60}n\varepsilon(d)mt = \frac{\dot{V}_E}{60}n\left[0.19+(0.83-0.19)\Big/\left(1+\exp\left(\frac{d\,(\mathrm{nm})-12.0}{24.0}\right)\right)\right]mt \tag{10}$$

where n is the aerosol mean number concentration in the inhalation chamber. It should be noted that the accuracy of ε is

mainly related to the uncertainty of $\dot{V}_E$ in the denominator of Eq. (8). However, the error in acquisition of *Dose* is not related to the uncertainty of $\dot{V}_E$ due to the product $\dot{V}_E\varepsilon$ entering into Eq. (10). There can be some error when estimating the lung-deposited dose in WB inhalation experiments using the quantity ε as determined in NOE chambers. The minute volume for animals immobilized in NOE chambers can differ from that for animals in WB chambers by about 20% (Currie et al., 1998; Hamelmann et al., 1997; Schaper & Brost, 1991; Vijayaraghavan, 1997). Therefore, we assume that the accuracy of Eq. (10) is also about 20%. The latter assumption is in agreement with the experimental measurements of the lung burdens after inhalation of TiO_2 and brass aerosol. It was shown by Yeh et al. (1990) that the difference in the lung burdens after inhalation in WB and NOE chambers is about 20% as well.

3.3. Hypotensive effect from nisoldipine nanoparticles inhalation

Each animal was used only once in the drug administration procedure. The rats were separated into four groups. The animals of the first group were subjected to the aerosol inhalation in WB or NOE chambers for 40 min; the animals of the second group were treated by i.v. injections of nisoldipine with the dose varied from 2.2×10^{-2} to 3.5×10^{-1} mg per kg bw, the animals of the third group were treated orally. The fourth group (untreated rats) was used as a control. The animals

Table 1
The nisoldipine aerosol inhalation results (group 1).

No.	Strain	P_0 (Torr)	P (Torr)	n (cm^{-3})	d_a (nm)	Chamber	Inhaled dose (mg/kg)	$(P_0-P)/P_0$
1.	WISTAR	142.6	112	9.3E6	123.1	WB	0.23	0.215
2.	WISTAR	141.5	112.8	1.1E7	120.1	WB	0.32	0.203
3.	WISTAR	138.8	123.4	1.2E7	110.7	WB	0.29	0.111
4.	WISTAR	134.5	120.3	1.1E7	115.2	WB	0.25	0.106
5.	WISTAR	144	121	7.6E6	98.7	WB	0.15	0.160
6.	WISTAR	139.7	123.5	9.5E6	84.8	WB	0.13	0.116
7.	WISTAR	144	132.8	9.4E6	92.6	WB	0.15	0.078
8.	WISTAR	128.4	103.8	1.0E7	129.5	WB	0.31	0.192
9.	WISTAR	128.3	120.2	1.1E7	106.1	WB	0.23	0.063
10.	WISTAR	136.8	124.6	1.1E7	130.3	WB	0.30	0.089
11.	WISTAR	124.7	102.7	1.3E7	78.8	WB	0.16	0.176
12.	WISTAR	138.3	103.8	1.3E7	161.7	WB	0.53	0.249
13.	WISTAR	136.5	107.3	1.2E7	85.3	WB	0.17	0.214
14.	WISTAR	139.3	101.6	1.3E7	116.4	WB	0.31	0.271
15.	WISTAR	132.7	100	1.4E7	128.6	WB	0.43	0.246
16.	WISTAR	121.7	108.7	1.4E4	25.3	WB	1.1E−5	0.107
17.	WISTAR	111.0	110.8	2.5E4	26.6	WB	2.4E−5	0.002
18.	WISTAR	126.2	102.3	4.7E6	35.2	WB	8.8E−3	0.189
19.	WISTAR	113.0	103.5	5.3E6	32.7	WB	8.2E−3	0.084
20.	WISTAR	136.0	136.8	1.35E6	20.51	WB	6.1E−4	−0.006
21.	WISTAR	135.2	137	1.1E6	20.71	WB	5.8E−4	−0.013
22.	WISTAR	127.5	129.4	4.0E6	32.17	WB	6.1E−3	−0.015
23.	WISTAR	125.3	128.3	4.5E6	56.33	WB	0.028	−0.024
24.	WISTAR	136.8	119.7	5.1E6	119.95	WB	0.14	0.125
25.	WISTAR	133.5	145	3.5E6	32.64	WB	5.5E−3	−0.086
26.	WISTAR	133	140.8	2.7E6	32.05	WB	3.7E−3	−0.059
27.	WISTAR	137.7	118.5	3.7E6	115.49	WB	0.092	0.139
28.	WISTAR	131.4	134.3	3.3E6	109.33	WB	0.078	−0.022
29.	WISTAR	132.3	129.2	4.2E6	140.93	WB	0.14	0.023
30.	WISTAR	141.0	122	1.6E6	77.2	NOE	0.014	0.134
31.	WISTAR	134.33	107	1.6E6	121.4	NOE	0.040	0.203
32.	WISTAR	156.75	120.25	1.6E6	202.5	NOE	0.39	0.233
33.	WISTAR	166	110.2	1.7E6	205	NOE	0.41	0.336
34.	ISIAH	228.58	169	5.6E6	88.4	WB	0.043	0.261
35.	ISIAH	196.5	152.5	5.3E6	113	WB	0.06	0.224
36.	ISIAH	206.5	171.8	5.3E6	139.2	WB	0.085	0.168
37.	ISIAH	210.8	157.8	5.1E6	139.7	WB	0.079	0.251
38.	ISIAH	207.7	199.7	5.5E6	132.2	WB	0.073	0.039
39.	ISIAH	193.8	193	3.0E6	25	WB	1.1E−3	0.004
40.	ISIAH	242.0	192.7	4.59E6	43.3	WB	6.8E−3	0.204
41.	ISIAH	183.3	182.5	4.6E6	56.5	WB	0.013	0.004
42.	ISIAH	207.3	165.8	5.0E6	44.4	WB	7.6E−3	0.200
43.	ISIAH	176	151	4.8E6	43.3	WB	6.4E−3	0.142

(P_0 and P are the systolic blood pressure values before and after the inhalation treatment, respectively; n is the aerosol number concentration, d_a is the aerosol arithmetic mean diameter.)

of the 4th group were exposed to pure air in WB chambers for 40 min without any other treatment. The lung-deposited dose for the first group inhalation experiments was determined using Eq. (10). The concentration n in this equation was set as a mean arithmetic between the chamber inlet and outlet aerosol concentrations as measured by the aerosol spectrometer. The mean mass m of aerosol particles was determined from the particle size distribution as measured by the aerosol spectrometer using nisoldipine density of 1.205 g/cm^3.

Tables 1–3 show the relative reduction of systolic blood pressure (i.e. the ratio between blood pressure reduction and the pressure before treatment) for the rats in groups 1–3. Fig. 14 compares the blood pressure reduction for WISTAR rats after the drug delivery in different ways vs. the body delivered dose. Open circles demonstrate the hypotensive effect after inhalation experiments. To avoid confusion, the nearby points for the group 1 measurements were averaged and presented in the graph by single points. One can see a significant increase of the blood pressure reduction at the lung delivered dose higher than 0.1 mg/kg. It is appropriate to mention that the group 4 (control) results (see Table 4) show that within the accuracy of several percent there is no reduction of the blood pressure after exposure to pure air. Important fact is that the lung delivered dose in WB inhalation experiments was determined using the lung deposition efficiency as determined in NOE experiments. Although, as discussed at the end of the previous section, the minute volume for animals immobilized in NOE chambers does not differ drastically from that for animals in WB chambers, it is useful to compare the dose–response effects for WB and NOE chambers with the lung delivered dose estimated in the same way using Eq. (10) (see circles and

Table 2
Results of intravenous treatment for the group 2 animals.

No.	Strain	P_0 (Torr)	P (Torr)	Injected dose (mg/kg)	$(P_0-P)/P_0$
1.	WISTAR	165	159	0.022	0.036
2.	WISTAR	113	113	0.022	0.0
3.	WISTAR	145	145	0.06	0.0
4.	WISTAR	127	133	0.06	−0.047
5.	WISTAR	159	133	0.22	0.163
6.	WISTAR	156	150	0.22	0.038
7.	WISTAR	154	127	0.22	0.175
8.	WISTAR	147	119	0.35	0.190
9.	WISTAR	152	122	0.35	0.197

Table 3
Results of oral treatment for the group 3 animals.

No.	Strain	P_0 (Torr)	P (Torr)	Deilvered dose (mg/kg)	$(P_0-P)/P_0$
1	WISTAR	105	107	0.0035	−0.02
2	WISTAR	108	112	0.0035	−0.04
3	WISTAR	109	98	0.0035	0.10
4	WISTAR	116	114	0.035	0.02
5	WISTAR	114	113	0.035	0.01
6	WISTAR	107	107	0.035	0.0
7	WISTAR	95	82	0.35	0.14
8	WISTAR	96	108	0.35	−0.13
9	WISTAR	104	92	0.35	0.12
10	WISTAR	99	100	0.35	−0.01
11	WISTAR	100	105	0.35	−0.05
12	WISTAR	104	110	0.35	−0.06
13	WISTAR	95	115	0.35	−0.21
14	WISTAR	101	99	0.35	0.02
15	WISTAR	98	92	1.0	0.06
16	WISTAR	116	95	1.0	0.18
17	WISTAR	100	83	1.0	0.17
18	WISTAR	102	84	1.0	0.18
19	WISTAR	102	89	1.0	0.12
20	WISTAR	100	98	1.0	0.02
21	WISTAR	108	109	3.5	−0.01
22	WISTAR	116	90	3.5	0.22
23	WISTAR	127	106	3.5	0.17
24	WISTAR	115	101	3.5	0.12
25	WISTAR	116	126	3.5	−0.09
26	WISTAR	97	71	10	0.27
27	WISTAR	102	90	10	0.11
28	WISTAR	99	72	35	0.27
29	WISTAR	99	64	35	0.35
30	WISTAR	99	79	35	0.20

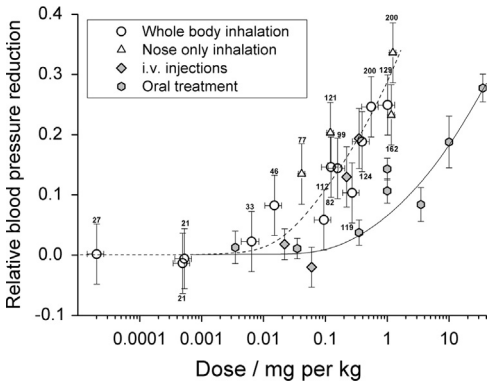

Fig. 14. Relative reduction of the arterial blood pressure $(P_0-P)/P_0$ for WISTAR rats (P_0 and P are pressures before and after treatment, respectively) vs. the dose delivered; circles – WB chamber; triangles – NOE chamber; diamonds – injections, and hexagons – oral delivery. Mean particle diameter is shown for each aerosol inhalation point. Dash and solid lines are eye guides for circles and hexagons, respectively.

Table 4
The blood pressure reduction for the group 4 animals (no treatment).

No.	Strain	P_0 (Torr)	P (Torr)	Chamber	$(P_0-P)/P_0$
1	WISTAR	121	126	WB	0.036
2	WISTAR	131	131	WB	0.0
3	WISTAR	140	137	WB	0.021
4	WISTAR	144	148	WB	−0.029
5	ISIAH	184	206	WB	−0.12

triangles). One can see that both dose–response relationships agree with each other within the experimental accuracy. Thus, Eq. (10) can be used for estimation of the lung delivered mass of nisoldipine for both WB and NOE chambers.

However, the systemic delivery depends on many factors that are difficult to control. It may be affected by where in the respiratory tract the drug is deposited, macrophage-mediated clearance, drug dissolution, translocation, blood absorption rate and others. Therefore, the lung delivered dose–response effect is compared with the i.v. dose–response dependence (compare circles with diamonds). One can see a good agreement between these two dose–response effects, which allows concluding that the lung delivered dose is approximately equal to the systemically delivered dose.

The results for oral treatment (group 3) are shown in Table 3 and Fig. 14 (hexagons). As seen from the graph, aerosol delivery is essentially more effective than oral administration, i.e. aerosol inhalation gives the same reduction of systolic blood pressure as oral treatment, with the body delivered dose about 100 times less for inhalation than for oral treatment. In other words, the same body-delivered dose results in quite different blood pressure reduction in inhalation and oral administrations. Thus, for example, for the body delivered dose of 1 mg per kg, nanoaerosol nisoldipine delivery results in the reduction of blood pressure four times higher than for traditional oral delivery.

The mean particle diameter is indicated for each inhalation administration point in Fig. 14. As one can see, the larger particle diameter corresponds to the higher dose, but it is hardly possible to find any correlation between particle diameter and antihypertensive action. The diameter–dose correlation is due to the fact that the dose augment was produced by an increase in evaporation temperature in the aerosol generator and, as a consequence, by an increase of the maternal substance evaporation rate. The augment of evaporation rate resulted in an increase in both the particle number concentration and the diameter.

It is of interest to see if any strain effect in the antihypertensive action can be observed. To this aim, the relative blood pressure reduction is compared for WISTAR and ISIAH rats in Fig. 15. One would conclude that within the experimental accuracy there is no difference in the blood pressure reduction effect for WISTAR and ISIAH rats.

3.4. Histology of the lungs

The histologic analysis was performed to observe possible hemodynamic abnormalities and pulmonary edema after the aerosol treatment. For this purpose, three animals were exposed to nanoparticles of $d=80$, 120 and 200 nm with the lung-deposited dose 0.04, 0.12 and 1.2 mg per kg bw, respectively. Both the control and aerosol-treated animals revealed the normal appearance of the lungs without any destructive and/or hemodynamic pathologic changes. The lungs showed numerous alveoli, had thin alveolar wall lined by simple squamous epithelium connected together through alveolar pores, which opened into alveolar sacs, alveolar ducts or

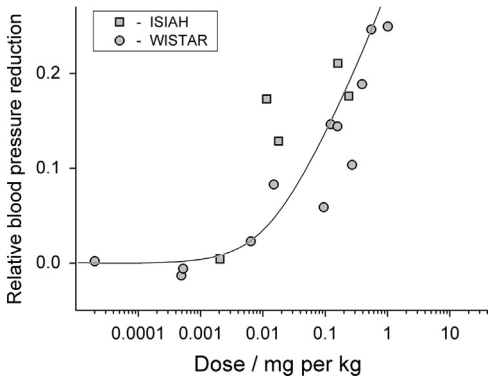

Fig. 15. Relative reduction of the arterial blood pressure vs. the lung delivered dose; circles – WISTAR, WB chamber; squares – ISIAH, WB chamber; solid line is an eye guide.

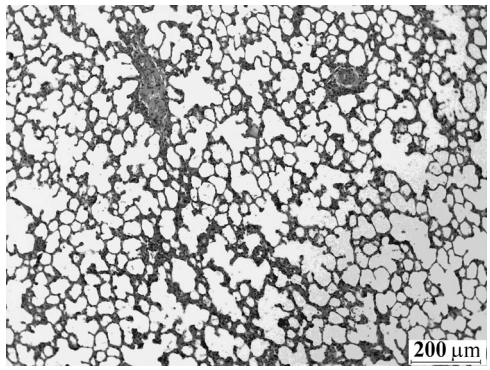

Fig. 16. Cross section of the lung from untreated WISTAR rat.

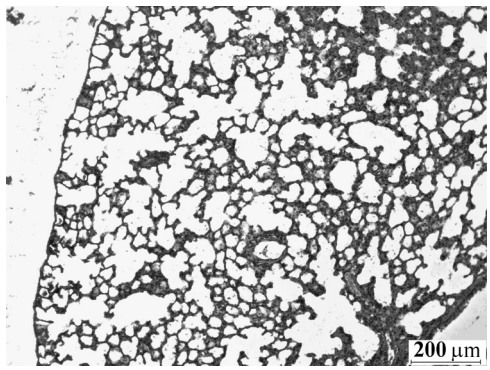

Fig. 17. Cross section of the lung from WISTAR rat treated with 120 nm nanoparticles.

respiratory bronchioles. The lobar bronchi mucosa was lined by high prismatic epithelium. The alveolar and terminal bronchial lumen did not show any emphysematous dilatation (Figs. 16 and 17).

4. Conclusions

The hypotensive action caused by the inhalation of nisoldipine nanoparticles 20–200 nm in diameter is investigated. To this end, an evaporation –condensation system is created which is able to generate aerosol nanoparticles within the size range 3–200 nm and number concentration 10^3–2×10^7 cm^{-3}. Chromatographic analysis showed that aerosol particles were chemically identical to the maternal substance (i.e. there was no thermal decomposition or oxidation during evaporation).

Using nose-only exposure chambers, we determined the lung deposition efficiency for WISTAR rats as a function of mean particle diameter (d_a) changing from about 0.6 for d_a=5 nm to about 0.2 for d_a within the range 100–160 nm.

It is concluded from the comparison between the lung delivered and i.v. dose–response effects that the lung delivered dose is approximately equal to the systemically delivered one.

It is found that within the experimental accuracy there is no difference in the blood pressure reduction effect for WISTAR and ISIAH rats, i.e. no strain effect in the antihypertension action is observed.

Inhalation experiments show that aerosol administration is substantially more effective than oral treatment, i.e. aerosol inhalation gives the same reduction of systolic blood pressure as oral treatment, with the body delivered dose for inhalation about 100 times smaller than that for oral treatment.

The histologic analysis is performed to observe possible hemodynamic abnormalities. Both the control and aerosol-treated animals reveal the normal appearance of lungs without any destructive and/or hemodynamic pathologic changes.

Acknowledgments

Financial support for this work was provided by the Siberian Branch of Russian Academy of Sciences (Interdisciplinary Integration Project 108) and the joint research project 3 between SB RAS and NSC Taiwan 2011–2014 and authors are grateful to S.G. Matveeva for help in experiments.

References

Agu, R.U., Ugwoke, M.I., Armand, M., Kinget, R., & Verbeke, N. (2001). The lung as a route for systemic delivery of therapeutic proteins and peptides. *Respiratory Research*, *2*, 198–209.

Ankilov, A., Baklanov, A., Colhoun, M., Enderle, K.-H., Gras, J., Junlanov, Yu., Kaller, D., Lindner, A., Lushnikov, A., Mavliev, R., McGovern, F., Mirme, A., O'Connor, T.C., Podzimek, J., Preining, O., Reischl, G.P., Rudolf, R., Sem, G.J., Szymanski, W.W., Tamm, E., Vrtala, A.E., Wagner, P.E., Winklmayr, W., & Zagaynov, V. (2002). Intercomparison of number concentration measurements by various aerosol particle counters. *Atmospheric Research*, *62*, 177–207.

Arms, A.D. & Travis, C.C. (1988). Reference Physiological Parameters in Pharmacokinetic Modeling, EPA report no. EPA/600/6-88/004. Washington, DC: U.S. Environmental Protection Agency, Office of Health and Environmental Assessment. Available from NTIS, Springfield, VA; PB88-196019.

Babatsikou, F., & Zavitsanou, A. (2010). Epidemiology of hypertension in the elderly. *Health Science Journal*, *4*, 24–30.

Bailey, M.M., & Berkland, C.J. (2009). Nanoparticle formulations in pulmonary drug delivery. *Medicinal Research Reviews*, *29*, 196–212.

Currie, W.D., van Schaik, S., Vargas, I., & Enhorning, G. (1998). Breathing and pulmonary surfactant function in mice 24 h after ozone exposure. *European Respiratory Journal*, *12*, 288–293.

Edwards, D.A., Valente, A.X., Man, J., & Tsapis, N. (2003). Recent advances related to the systemic delivery of therapeutic molecules by inhalation. In A.J. Hickey (Ed.), *Pharmaceutical Inhalation Aerosol Technology*. CRC Press: New York, pp. 541–550.

Fuchs, N.M. (1964). *The Mechanics of Aerosol*. Pergamon Press: Oxford.

Gagnadoux, F., Pape, A.L., Lemarie, E., Lerondel, S., Valo, I., Leblond, V., Racineux, J.-L., & Urban, T. (2005). Aerosol delivery of chemotherapy in an orthotopic model of lung cancer. *European Respiratory Journal*, *26*, 657–661.

Hamelmann, E., Schwarze, J., Takeda, K., Oshiba, A., Larsen, G.L., Irvin, C.G., & Gelfand, E.W. (1997). Noninvasive measurement of airway responsiveness in allergic mice using barometric plethysmography. *American Journal of Respiratory and Critical Care Medcine*, *156*, 766–775.

Heyder, J. (2004). Deposition of inhaled particles in the human respiratory tract and consequences for regional targeting in respiratory drug delivery. *Proceedings of the American Thoracic Society*, *1*, 315–320.

Hinds, W.C. (1999). *Aerosol Technology. Properties, Behavior, and Measurement of Airborn Particles* 2nd ed). John Wiley & Sons, Inc.: New York.

Hofmann, W., Asgharian, B., Bergmann, R., Anjilvel, S., & Miller, F.J. (2000). The effect of heterogeneity of lung structure on particle deposition in the rat lung. *Toxicological Sciences*, *53*, 430–437.

Hussain, M., Madl, P., & Khan, A. (2011). Lung deposition predictions of airborne particles and the emergence of contemporary diseases Part-I. *theHealth*, *2*, 51–59.

Jaques, P.A., & Kim, C.S. (2000). Measurement of total lung deposition of inhaled ultrafine particles in healthy men and women. *Inhalation Toxicology*, *12*, 715–731.

Kirsh, A.A., Stechkina, I.B., & Fuchs, N.A. (1975). Efficiency of aerosol filters made of ultrafine polydisperse fibres. *Journal of Aerosol Science*, *5*, 119–124.

Labiris, N.R., & Dolovich, M.B. (2003). Pulmonary drug delivery. Part I: Physiological factors affecting therapeutic effectiveness of aerosolized medications. *Journal of Clinical Pharmacology*, *56*, 588–599.

Labiris, N.R., & Dolovich., M.B. (2003). Pulmonary drug delivery. Part I: Physiological factors affecting therapeutic effectiveness of aerosolized medications. *Journal of Clinical Pharmacology*, *56*, 588–599.

Laube, B.L. (2005). The expanding role of aerosols in systemic drug delivery, gene therapy, and vaccination. *Respiratory Care*, *50*, 1161–1176.

Maghraby, G.M.El, & Elsergany, R.N. (2014). Fast disintegrating tablets of nisoldipine for intra-oral administration. *Pharmaceutical Development and Technology*, *19*, 641–650.

Oberdörster, G., Oberdörster, E., & Oberdörster, J. (2005). Nanotoxicology: an emerging discipline evolving from studies of ultrafine particles. *Environmental Health Perspectives*, *113*, 823–839.

Onischuk, A.A., Tolstikova, T.G., Sorokina, I.V., Zhukova, N.A., Baklanov, A.M., Karasev, V.V., Borovkova, O.V., Dultseva, G.G., Boldyrev, V.V., & Fomin, V.M. (2009). Analgesic effect from ibuprofen nanoparticles inhaled by male mice. *Journal of Aerosol Medicine and Pulmonary Drug Delivery*, *22*, 245–253.

Onischuk, A.A., Tolstikova, T.G., Sorokina, I.V., Zhukova, N.A., Baklanov, A.M., Karasev, V.V., Dultseva, G.G., Boldyrev, V.V., & Fomin, V.M. (2008). Anti-inflammatory effect from indomethacin nanoparticles inhaled by male mice. *Journal of Aerosol Medicine and Pulmonary Drug Delivery* (21), 231–244.

Patton, J.S., Fishburn, C.S., & Weers, J.G. (2004). The lungs as a portal of entry for systemic drug delivery. *Proceedings of the American Thoracic Society*, *1*, 338–344.

Prisant, L.M., & Elliott, W.J. (2003). Drug delivery systems for treatment of systemic hypertension. *Clinical Pharmacokinetics*, *42*, 931–940.

Rabinowitz, J.D., Lloyd, P.M., Munzar, P., Myers, D.J., Cross, S., Damani, R., Quintana, R, Spyker, D.A., Soni, P., & Cassella, J.V. (2006). Ultra-fast absorption of amorphous pure drug aerosols via deep lung inhalation. *Journal of Pharmaceutical Sciences*, *95*, 2438–2451.

Rabinowitz, J.D., Wensley, M., Lloyd, P., Myers, D., Shen, W., Lu, A., Hodges, C., Hale, R., Mufson, D., & Zaffaroni, A. (2004). Fast onset medications through thermally generated aerosols. *Journal of Pharmacological Experiment and Therapy*, *309*, 769–775.

Rabinowitz, J.D., & Zaffaroni, A.C. (2004). *Delivery of physiologically active compounds through an inhalation route*. United States Patent 0185002.

Ruge, C.A., Kirch, J., & Lehr, C.-M. (2013). Pulmonary drug delivery: from generating aerosols to overcoming biological barriers – therapeutic possibilities and technological challenges. *The Lancet Respiratory Medicine*, *1*, 402–413.

Schaper, M., & Brost, M.A. (1991). Respiratory effects of trimellitic anhydride aerosols in mice. *Archives of Toxicology*, *65*, 671–677.

Tolstikova, T.G., Onischuk, A.A., Sorokina, I.V., Baklanov, A.M., Zhukova, N.A., Karasev, V.V., Boldyrev, V.V., Fomin, V.M., Khvostov, M.V., Bryzgalov, A.O., & Tolstikov, G.A. (2013). Research and development of a new safe form of drugs. In L.S. Ruzer, & N.H. Harley (Eds.), *Aerosols Handbook. Measurement, Dosimetry, and Health Effects* (2nd ed). CRC Press: Boca Raton, New York, pp. 249–284.

Vijayaraghavan, R. (1997). Modifications of breathing pattern induced by inhaled sulphur mustard in mice. *Archives of Toxicology*, *71*, 157–164.

White, W.B. (2007). Pharmacologic agents in the management of hypertension – nisoldipine coat-core. *The Journal of Clinical Hypertension*, *9*, 259–266.

Wong, B.A. (2007). Inhalation exposure systems: design, methods and operation. *Toxicologic Pathology*, *35*, 3–14.

Yeh, H.C., Snipes, M., Eidson, A.F., & Hobbs, C.H. (1990). Comparative evaluation of nose-only versus whole-body inhalation exposures for rats-aerosol characteristics and lung deposition. *Inhalation Toxicology*, *2*, 205–221.